2018

IMPORTANCE OF GROWTH RATE ON HG AND PCB BIOACCUMULATION IN FISH

Jiajia Li
University of Windsor

G. Douglas Haffner
University of Windsor

Gordon Paterson
Michigan Technological University

David M. Walters
U.S. Geological Survey

Michael D. Burtnyk
CH2M Hill Energy, Canada

See next page for additional authors

IMPORTANCE OF GROWTH RATE ON HG AND PCB BIOACCUMULATION IN FISH

Jiajia Li[a]*, G. Douglas Haffner[a], Gordon Paterson[b], David M. Walters[c], Michael D. Burtnyk[d], Ken G. Drouillard[a]

a. Great Lakes Institute for Environmental Research, University of Windsor, 401 Sunset Avenue, Windsor, Ontario, Canada N9B 3P4

b. Biological Sciences, Michigan Technological University, 1400 Townsend Drive, Houghton, Michigan, United States 49931-1295

c. U.S. Geological Survey, Fort Collins Science Center, 2150 Centre Avenue, Fort Collins, Colorado, United States 80526-8118

d. CH2M Hill Energy Canada, 540 12 Ave SW, Calgary, Alberta, Canada T2R 0H4

*Corresponding author: Jiajia Li Email: li111137@uwindsor.ca

ABSTRACT

To evaluate the effect of fish growth on mercury (Hg) and polychlorinated biphenyls (PCBs) bioaccumulation, a non-steady state toxicokinetic model, combined with a Wisconsin bioenergetics model, was developed to simulate Hg and PCB bioaccumulation in Bluegill (*Lepomis macrochirus*). The model was validated by comparing observed versus predicted Hg and PCB 180 concentrations across 5 age classes from five different waterbodies across North America. The non-steady state model generated accurate predictions for Hg and PCB bioaccumulation in three of five waterbodies: Apsey, Sharbot and Stonelick Lake. The poor performance of the model for the Detroit River and Lake Hartwell, which were two well-known contaminated sites with possibly high heterogeneity in spatial contamination, was attributed to changes in the feeding behavior and/ or change in prey contamination. Model simulations indicate that growth dilution is a major component of contaminant bioaccumulation patterns in fish especially during early life stages and was predicted to be more important for hydrophobic PCBs compared to Hg. Simulations which considered tissue specific growth provided some improvement in model performance particularly for PCBs in fish populations which exhibited changes in their whole body lipid content with age. Higher variation in lipid growth compared with that of lean dry protein was also observed between different bluegill populations which

partially explains the greater variation in PCB bioaccumulation slopes compared with Hg across sampling sites.

Keywords: Persistent Organic Pollutants, Mercury, Toxicokinetics, Bioenergetics, Growth Dilution

INTRODUCTION

Mercury (Hg) and polychlorinated biphenyls (PCBs) are globally dispersed pollutants with high potential for bioaccumulation in aquatic species (McIntyre et al. 2007). Both of these chemical groups present human health risks due to exposure through the consumption of contaminated fish and shellfish (Watanabe et al. 2003). In order to improve risk assessment predictions and develop appropriate mitigation solutions that help reduce the bioaccumulation of these toxic pollutants in biota and minimize exposure risks to higher level consumers, it is imperative to accurately predict Hg and PCB bioaccumulation in fish. Despite Hg and PCBs being the most frequent cause of fish consumption restrictions (US EPA 2010 &2014; OMOE 2016), most research typically focus on one of these legacy pollutants. Direct comparisons of Hg and PCB bioaccumulation dynamics are rare assumedly due to the different instrumentation requirements for analysis, as well as differences in their environmental speciation, fate, and the physiological mechanisms regulating their assimilation, biotransformation and elimination pathways (Mason et al. 1995; Gobas et al. 1999). Yet, there are many commonalities among the general bioaccumulation characteristics for these two pollutants such that common predictive models for understanding their bioaccumulation by fish have been proposed (Li et al. 2015). Toxicokinetic bioaccumulation models adopt mass balance principles and use experimentally calibrated rate coefficients to describe pollutant uptake from water and food, whole body elimination, and growth dilution (Trudel and Rasmussen, 2001; McLeod et al. 2016). However, toxicokinetic rate constants determined via controlled laboratory experiments are often specific to experimental conditions and the test species utilized which can lead to inaccurate predictions when such coefficients are extrapolated to field conditions.

To better address species responses to field conditions, toxicokinetic models have been coupled with species specific bioenergetic sub-models that address animal metabolic rate and growth responses to varying environmental conditions. Such bioenergetics models were developed to predict food consumption, gill ventilation, fecal egestion, and growth rates over the range of environmental conditions that an individual or population may experience at daily, seasonal, and annual temporal scales (Kitchell and Stewart, 1977; Trudel and Rasmussen, 2006). Bioenergetic models have been calibrated for a wide variety of fish species thereby providing the capacity to predict changes in fish physiological processes across a wide range of temperature optima and allometric scaling coefficients (Madenjian et al. 2006; Holker and Haertel, 2004). Thus, coupled bioenergetic-toxicokinetic models have the advantage of being scalable to the different environmental conditions that fish populations are likely to experience over their

natural habitat range with life history characteristics such as ontogenetic diet shifts being easily incorporated into the model structure (Drouillard et al. 2009). Further, combined bioenergetic-toxicokinetic models provide the capacity to predict pollutant bioaccumulation under the assumption of non-steady state bioaccumulation which is frequently the condition for highly persistent and hydrophobic pollutants such as Hg (Li et al. 2015) and PCBs (Paterson et al. 2007; McLeod et al. 2016).

Toxicokinetic models developed for predicting Hg and PCB bioaccumulation are generally sensitive to fish growth rates as tissue growth (dilution) and weight loss (bioamplification) represent key factors for understanding differences in pollutant bioaccumulation within and among fish populations (Simoneau et al. 2005; Paterson et al. 2007; Daley et al. 2014). However, many food web bioaccumulation models assume fish growth to be constant over an animal's life (Gobas 1995), yet fish growth in nature is both time and temperature dependent such that growth rates vary with age and season (Ricker 1979). Further, for Hg and PCBs, protein and lipid in tissues, respectively, dictate the maximum capacities for an individual to bioaccumulate these pollutants (Mackay, 1982; Roesijadi, 1992). As such, differences in the rates of protein vs. lipid growth, i.e. the rate at which each of these tissue pools grow independent of measured whole body mass changes, could have contrasting effects of growth dilution on Hg and PCB potentially resulting in a decoupling of bioaccumulation trajectories between these pollutants.

In most bioaccumulation studies, growth is typically representative of whole body mass with individual tissue growth rates considered proportional to such somatic growth (Trudel and Ramussen, 2006; Drouillard et al. 2009). However, protein mass has a much stronger correlation to changes in whole body growth while the relationships between lipids and whole body mass are frequently weaker due to the supporting role of lipids as an energy reserve in many fish species (Overturf et al. 2016). Finally, growth itself has an energetic cost, requiring additional food consumption to generate new tissue and satisfy routine metabolic rate. Therefore, growth dilution cannot be examined independently of chemical intake rates via food consumption. Bioenergetic models are thus necessary to tease out growth dilution effects while also considering associated changes in chemical intake rate.

The present study was developed to evaluate the effect of growth dilution on Hg and PCB bioaccumulation in different populations of Bluegill (*Lepomis macrochirus*) using a non-steady state bioenergetic-toxicokinetic bioaccumulation model. Bluegills are a common fish species in North America. They inhabit shallow waters of the littoral zone, feed primarily on nearshore invertebrates and exhibit minimal ontogenetic diet shifts compared to large piscivores (Paterson et al. 2006). Their affiliation with nearshore waters makes them subject to large seasonal changes in water temperature anticipated to influence annual growth owing to large seasonal changes in specific growth rate. These features make bluegills an ideal model species to evaluate growth dilution effects on contaminant bioaccumulation. Fish, aged 0 to 5 years, were collected from a set of five waterbodies over a latitudinal gradient ranging from 34° to 46° north

latitude (Figure 1). This ensured that each population was subject to different thermal regimes known to impact annual fish growth. In addition, two of the sampling sites, Lake Hartwell and the Detroit River, are known to be contaminated systems. Lake Hartwell is a Superfund site owing to PCB releases from a capacitor manufacturer near Pickens, SC (Bzdusek, et al. 2006) while the Detroit River is designated as a Great Lakes Area of Concern with both PCBs and Hg listed as priority pollutants (Drouillard et al. 2006; Szalinska et al. 2006). Fish from different baseline contamination sites can assist with validating the effect of growth on various bioaccumulation scenarios.

The bioenergetic-toxicokinetic bioaccumulation model was used to simulate Hg and PCB accumulation with age in fish for each population using field measured growth rates and contrasted with empirical bioaccumulation trends. Two different simulations were contrasted for their predictive capability. Simulation 1, assumed lipid and protein compartment growth rates were proportional to whole body growth to predict Hg and PCB bioaccumulation for each population. Because most of the lean dry tissue (approximate 90%) is protein (Overturf et al. 2016), lean dry weight (excluding moisture and lipid) was used to represent protein weight in the present study. Simulation 2 applied lipid and protein compartment growth rates of specific age and population. Goodness of fit tests were used to discriminate between the simulations and to test the hypothesis that a common bioenergetic-toxicokinetic bioaccumulation model incorporating age and/or tissue specific growth dilution can account for deviations in bioaccumulation patterns of Hg and PCBs in fish.

METHODS

Sampling. Multiple sizes (0.1 to 130.9 g) of Bluegill were collected in October, 2006 from Apsey Lake (46.2268° N, 81.7689° W), Sharbot Lake (44.7667° N, 76.6833° W), the Detroit River (42.2167° N, 83.1333° W), and Stonelick Lake (39.2203 ° N, 84.0725° W). Bluegills were also sampled in June, 2006 from Lake Hartwell (34.4652° N, 82.8455° W). As shown in Figure 1, Apsey Lake, Sharbot Lake, and the Detroit River are located in Canada, while Stonelick Lake and Lake Hartwell are located in US. Fish were stored at -30ºC prior to dissection. Biological data, including wet weight and total lengths, were catalogued. Otoliths were removed to determine the age of each individual. Each individual was then homogenized and analyzed for total Hg (THg), PCBs (PCB 17/18, 28/31, 33, 44, 49, 52, 70, 74, 87, 95, 99, 101, 110, 118,128, 153, 105/132, 138, 149,151/82, 158, 156/171, 170, 177, 180, 183, 187, 191, 194, 199, 195/208, 205, 206, and 209), carbon and nitrogen stable isotopes.

Laboratory Analysis. Laboratory analysis was carried out at the Great Lake Institute for Environmental Research, University of Windsor. Standard operating procedures, which were accredited through the Canadian Association for Laboratory Analysis (CALA), were followed throughout the lab analysis. The procedures for THg, PCBs, nitrogen and carbon stable isotope analysis, as well as age determination are described in Supplemental Material. Because most of

the THg (>95%) in fish is MeHg (Bloom 1992), this study assumed that THg concentration equals MeHg concentration. In addition, changes in nitrogen stable isotope signatures were used as indicators of changes in the diets of fish populations with age, and changes in carbon stable isotopes were used as indicators of habitat changes (Burtnyk et al. 2009).

Water temperature. Annual water temperature cycle was estimated for each of the five waterbodies based on local air temperature, due to the unavailability of *in situ* field data. The detailed information regarding water temperature model is described in Supplemental Material.

Growth Model. Two growth scenarios were established from the measured whole body weight, lipid%, and lean dry weight% of each population and each age class. Scenario 1 was based on the whole body growth measured in each population. The proportion of lean dry protein and lipid was assumed to be constant and scaled to measured changes in whole body weight observed for each population across all age classes. Fish growth is dependent on water temperature (Berg and Bremset, 1998), and therefore daily growth was apportioned such that the highest daily growth was achieved during the summer periods of warmest water temperatures and slowest during the winters. The whole body daily growth increment ($\Delta W_{wb.d}$; g) was calculated for each age class and population according to:

$$\Delta W_{wb,d} = \left(\bar{W}_{wb,y+1} - \bar{W}_{wb,y}\right) \cdot \left(\frac{T_d}{\sum_{d=1}^{365} T_d}\right) \quad (1)$$

Where $\bar{W}_{wb,y+1}$ and $\bar{W}_{wb,y}$ are the mean body weights (g) of fish from a given population for the next age class and mean body weight (g) of fish from the same lake for the current age class being simulated, T_d is the water temperature (°C) for the day of year of the simulation derived from the water temperature submodel and $\sum_{d=1}^{365} T_d$ is the cumulative degree days over a model year for a given lake. For each population, the mean % lipid and % lean dry weight across all age classes from a given population was computed and applied to the daily whole body weight increment determined from Eq. 1 to compute the daily change in lipid and protein pool weights.

Scenario 2 allowed lipid and protein composition to vary according to measured changes in proximate tissue composition between year classes in each population. Whole body weight growth changes were measured according to the same procedure described in Eq. 1. Daily growth increments of lipids ($\Delta W_{lip,d}$) and protein ($\Delta W_{pro,d}$) were generated in an analogous fashion to whole body weight increments. Thus for lipids, the daily weight increment was given as:

$$\Delta W_{lip,d} = \left(\bar{W}_{lip,y+1} - \bar{W}_{lip,y}\right) \cdot \left(\frac{T_d}{\sum_{d=1}^{365} T_d}\right) \quad (2)$$

Where $\bar{W}_{lip,y+1}$ and $\bar{W}_{lip,y}$ are the mean total lipid weights (g) of fish from a given population for the next age class and mean total lipid weight (g) of fish from the same lake for the current

year class of simulation. The identical procedure was used to estimate daily weight increments ($\Delta W_{pro,d}$) of lean dry protein.

The daily growth rate of lean dry protein ($k_{g,pro}$) and lipid weight($k_{g,lip}$) was also determined using the same procedure by factoring in time (t, d), according to:

$$k_{g,lip} = \frac{W_{lip,d+1} - W_{lip,d}}{t \cdot W_{lip,d}} \quad (3)$$

Bioenergetic Model. The Wisconsin bioenergetic model for Bluegill was applied to predict daily food consumption rates, gill ventilation volumes, and fecal production rates for each day of the simulation. The model was similar to that described by Drouillard et al. (2009), with a few changes in the algorithm based on the Bluegill physiological parameters. Food consumption rates (C; kJ·g^{-1}·d^{-1}) were calculated according to:

$$C = \frac{(G_L + G_P) + R \cdot D_{O_2} + SDA + U}{E_C} \quad (4)$$

where G_L is growth of somatic lipid (kJ·g^{-1}·d^{-1}), G_P is growth of somatic protein (kJ·g^{-1}·d^{-1}; measured as lean dry weight), R is specific rate of respiration (g·g^{-1}·d^{-1}), D_{O2} is the oxycalorific coefficient for converting oxygen respired to energy of fish (14.30 kJ·g^{-1}O$_2$; Norstrom et al. 1976), SDA is the specific dynamic action (kJ·g^{-1}·d^{-1}), U is energy lost to excretion (kJ·g^{-1}·d^{-1}), and E_C is the energy assimilation efficiency from food (unitless).

G_L and G_P were calculated based on the aforementioned growth models by multiplying the energy value of the corresponding tissue with the daily weight increment estimated for each tissue type. Lipid carries an energetic value of 39.3 kJ·g^{-1} and protein carries an energetic value of 18.0 kJ·g^{-1} (Drouillard et al 2009).

R is calculated using Equation 2 of the Wisconsin bioenergetic model version 3 (Hanson et al. 1997) described for Bluegill and is summarized as follows:

$$R = 0.0154 \cdot W_{wb,d}^{-0.2} \cdot \left[\left(\frac{36 - T_d}{9} \right)^{2.04} \cdot e^{\left\langle 2.04 \cdot \left(1 - \left(\frac{36 - T_d}{9} \right) \right) \right\rangle} \right] \cdot A \quad (5)$$

Where $W_{wb,d}$ is fish body weight for a given day (g), A is activity multiplier (unitless), which is usually between 1 to 2 (A=1, 1.5, and 2 was each applied in this study to simulate 3 activity levels). SDA and U were estimated from the following equations:

$$SDA = 0.172 \cdot (R \cdot D_{O_2} + |G_L| + |G_P|) \quad (6)$$

$$U = 0.0253 \cdot T_d^{0.58} \cdot e^{-0.299} \cdot (R \cdot D_{O_2} + |G_L| + |G_P|) \quad (7)$$

E_C was estimated for the diet according to Arnot and Gobas (2004):

$$E_C = \frac{39.3 \cdot X_{L,D} \cdot E_L + 18.0 \cdot X_{P,D} \cdot E_P}{ED_{Food}} \quad (8)$$

where $X_{L,D}$ and $X_{P,D}$ refer to the mass fraction of lipid and protein in the diet (unitless, assumed to be equal to the YOY composition), E_L and E_P are assimilation efficiencies of dietary lipid and protein (unitless, E_L =0.92 and E_P =0.60 were applied according to Arnot and Gobas, 2004), the coefficients 39.3 and 18.0 are the energy density (kJ·g^{-1}) of lipid and protein, and ED_{Food} is the total energy density (kJ·g^{-1}) of food, which is calculated as:

$$ED_{Food} = 39.3 \cdot X_{L,D} + 18.0 \cdot X_{P,D} \quad (9)$$

The consumption rate from eq 4 is converted into a mass flow (Q_C; g food·g^{-1}·d^{-1}) by considering the energy density (ED_{Food}; kJ·g^{-1}) of consumed food;

$$Q_C = \frac{C}{ED_{Food}} \quad (10)$$

The fecal egestion rate (Q_{EX}; g feces·g^{-1}·d^{-1}) and gill ventilation rate (Q_V; mL·g^{-1}·d^{-1}) are required as inputs to the toxicokinetic submodel for PCB simulation. Q_{EX} and Q_V are calculated as:

$$Q_{EX} = Q_C \cdot (1 - (X_{L,D} \cdot E_L + X_{P,D} \cdot E_P)) \quad (11)$$

$$Q_V = \frac{R \cdot D_{O_2} + SDA + U}{D_{O_2} \cdot C_{O_2} \cdot E_{O_2} \cdot W_{wb,d}} \quad (12)$$

Where C_{O2} is the concentration of oxygen dissolved in water (g O_2·mL^{-1}) and E_{O2} is the oxygen extraction efficiency (0.60 unitless; McKim et al. 1985) across the gills. Oxygen concentrations were assumed to be saturated and estimated by:

$$C_{O_2} = \frac{14.45 - 0.413 \cdot T_d + 5.56 \times 10^{-3} \cdot T_d^{\,2}}{1000000} \quad (13)$$

Toxicokinetic Model. Since Hg uptake from water only represents 0.1% of the Hg accumulated in fish, aqueous uptake is considered negligible (Hall et al. 1997). The daily change in Hg lean dry concentration was modeled by:

$$\frac{dC_p}{dt} = \frac{C_{d,Hg} \cdot Q_C \cdot W_{wb,d} \cdot AE_{Hg}}{W_{pro,d}} - \left(k_{tot} + k_{g,pro}\right) \cdot C_p \quad (14)$$

Where C_P is the Hg lean dry weight concentration (ng·g^{-1}) in the animal, $C_{d,Hg}$ is the Hg concentration in fish diet (ng·g^{-1}), AE_{Hg} is the Hg assimilation efficiency (unitless), k_{tot} is the whole body Hg elimination rate coefficient that represents all elimination pathways including chemical loss via respiration, via urine, feces, and metabolic biotransformation (g·g^{-1}·d^{-1}), and

$k_{g,pro}$ is the fractional growth of the protein compartment experienced over the daily increment (d^{-1}).

The AE_{Hg} was set equal to 90% (Leaner and Mason, 2004, Li et al. 2015). $C_{d,Hg}$ of each site was estimated using Hg concentration of YOY from the corresponding site divided by a biomagnification factor (BMF). A calibrated BMF for each location was estimated using Hg concentration of YOY divided by the model best fit $C_{d,Hg}$, which was obtained by fitting $C_{d,Hg}$ into the bioaccumulation model to achieve the best fit to field data. Calibrated BMFs from each lake were combined to generate a mean Bluegill BMF. The mean inter-lake BMF was then used for each lake to estimate lake specific $C_{d,Hg}$ values as the model input. k_{tot} for multiple species were taken from previous literature studies (Trudel and Rasmussen, 1997), and the routine metabolic rate for each species was estimated by the Wisconsin bioenergetic model. The mean ratio of k_{tot} to metabolic rate from the literature calibration data set was then used to estimate a daily k_{tot} for Bluegill based on its metabolic rate estimated for a given simulation day. The estimated conversion factor for Bluegill was treated as:

$$k_{tot} = \left((G_L + G_P) + R \cdot D_{O_2} + SDA + U\right) \cdot 0.0659 \quad (15)$$

For PCB simulations, PCB 180 was used as a representative congener as a result of its high hydrophobicity and commonality in elimination rate coefficient compared to Hg (Li et al. 2015). Because lean dry protein has 5% of the lipid partitioning capacity for PCB (Debruyn et al. 2007), the PCB concentration is normally expressed on a lipid-equivalent basis. According to the uptake and elimination mechanisms, the daily change in PCB lipid-equivalent concentration is:

$$\frac{dC_L}{dt} = \frac{C_{d,PCB} \cdot Q_C \cdot W_{wb,d} \cdot AE_{PCB} + C_W \cdot W_{wb,d} \cdot Q_V \cdot E_w}{W_{L,d}} - \left(k_2 + k_{EX} + k_{g,lip}\right) \cdot C_L \quad (16)$$

Where C_L is the lipid-equivalent PCB concentration ($ng \cdot g^{-1}$ lipid) in the animal, $C_{d,PCB}$ is the PCB concentration in fish diet ($ng \cdot g^{-1}$), Q_C is the consumption rate (g food$\cdot g^{-1} \cdot d^{-1}$) from eq 12, AE_{PCB} is the PCB assimilation efficiency (unitless), $W_{L,d}$ is the lipid equivalent weight ($W_{lip,d}$+0.05$\cdot W_{pro,d}$) (g), C_w is the PCB concentration in water ($ng \cdot g^{-1}$), Q_V is the gill ventilation rate ($m \cdot g^{-1} \cdot d^{-1}$) from eq 14, E_w is the chemical exchange efficiency across the gills (unitless), and k_2, k_{EX}, and $k_{g,lip}$ (Eq. 3) refer to mass elimination rate constants (d^{-1}) for chemical depuration across the gills, feces, and daily fractional lipid growth increment (d^{-1}).

The AE_{PCB} was set equal to 60% (Liu et al. 2010). $C_{d,PCB}$ of each location was calibrated using PCB concentration of YOY from the corresponding site divided by a BMF. The BMF was obtained by the same procedure as for Hg. Under the assumption that PCB lipid concentration in YOY fish ($C_{YOY,PCB}$) is at thermodynamic equilibrium with water PCB concentration, C_w is calculated according to:

$$C_w = \frac{C_{YOY}}{K_{OW}} \quad (17)$$

Where K_{OW} is octanol/water partition coefficient of the chemical (unitless). The gill elimination rate constant is calculated as:

$$k_2 = \frac{E_w \cdot Q_V}{K_{BW}} \tag{18}$$

Where K_{BW} is the biota/water partition coefficient (unitless), which is estimated as:

$$K_{BW} = X_{L,B} \cdot K_{OW} + 0.05 \cdot X_{P,B} \cdot K_{OW} \tag{19}$$

Where $X_{L,B}$ and $X_{P,B}$ is the fraction of lipid and lean dry protein in the animal (unitless). The recommended algorithm for estimating E_w is given as:

$$E_w = (1.85 + \frac{155}{K_{OW}})^{-1} \tag{20}$$

Fecal elimination rate constants (k_{EX}) were estimated by:

$$k_{EX} = \frac{E_{EX} \cdot Q_{EX}}{K_{B.EX}} \tag{21}$$

Where E_{EX} is the PCB organism/fecal exchange efficiency (assumed to be equal to AE_{PCB}), Q_{EX} is derived from eq 13, and $K_{B,EX}$ is the biota/feces partition coefficient (unitless).

$$K_{B,EX} = \frac{X_{L,B} + 0.05 \cdot X_{P,B}}{X_{L,EX} + 0.05 \cdot X_{P,EX}} \tag{22}$$

Where $X_{L,EX}$ and $X_{P,EX}$ is the fraction of lipid and lean dry protein in the feces (unitless).

Following model validation against empirical data, model simulations were interpreted to provide further insight into the relative contributions of growth and whole body chemical elimination to chemical concentrations in fish. The fraction of chemical retained by fish was calculated for each age class and population as the ratio of total chemical mass in fish divided by the total amount of chemical assimilated by fish from food (and water for PCBs) over time. The magnitude of k_g relative k_{tot} was then contrasted to compare growth dilution and chemical elimination. For example, under the condition where $k_g = k_{tot}$, growth dilution and chemical elimination are of equal importance to chemical bioaccumulation and the fraction of chemical retained will be twice that of an equivalent simulation where k_g is negligible in magnitude relative to k_{tot}. This allowed comparing the effect of growth dilution vs whole body elimination between contaminants and between fish populations. For interpretation purposes, k_g and k_{tot} were expressed as ranges in daily rate coefficient values generated by the model over the time from each simulation.

Data Analysis. For all data analysis, PCB concentrations were expressed on a lipid-equivalent weight basis, and THg concentrations were expressed in units of $ng \cdot g^{-1}$ lean dry weight. Analysis of variance (ANOVA) was used to test for differences among sampling sites in THg concentration and sum PCB concentration. Linear regression analysis was performed with ANOVA to test whether total wet weight, lean dry weight, lipid weight, THg concentration, PCB 180 concentration, and carbon and nitrogen stable isotope values were significantly related to fish age. Linear regression was also performed between measured and predicted chemical (PCB 180 and THg) concentrations. T-tests were used to test if the constant was significantly different from 0, and if slope was significantly different from 1. Prior to using parametric tests, normality and homogenous variance were tested by Kolmogorov-Smirnov and Levene's tests. Data that failed the normality test were $\log_{10}$ transformed. All statistical analyses were performed using IBM SPSS version 20 (IBM Corp., USA).

RESULTS

Hg and PCB concentrations in Bluegill. Table 1 presents the summarized biological data, as well as THg and sum PCB concentrations. Significantly higher mean total length was found in Bluegill from the most southern lake, Lake Hartwell (9.6 ± 0.4 mm), compared with fish from northern lakes including Apsey Lake (7.5 ± 0.4 mm) and Sharbot Lake (7.8 ± 0.4 mm) (ANOVA, $p<0.05$). The mean body weights of Bluegill from the Detroit River (18.5 ± 3.3 g) and Lake Hartwell (16.9 ± 2.0 g) were significantly higher compared with those from Apsey Lake (9.6 ± 1.1 g) and Sharbot Lake (10.4 ± 1.5 g) (ANOVA, $p<0.05$). These results indicate that Bluegill from southern waterbodies tended to have larger body size than those from northern waterbodies.

The THg lean dry weight concentration was positively related to age for fish from Apsey Lake, Sharbot Lake, Stonelick Lake, and Lake Hartwell (linear regression, $p<0.05$), but no significant relationship between THg lean dry concentration and age was found for fish from Detroit River. For PCBs, there were positive relationships between the sum PCB lipid-equivalent concentration and age for fish from Detroit River and Lake Hartwell (linear regression, $p<0.05$), but no significant relationship between sum PCB lipid-equivalent concentration and age for fish from Apsey Lake, Sharbot Lake, and Stonelick Lake. The field data commonly showed changes in chemical concentration with age, indicating that chemical accumulation in these fish did not achieve steady state across the age groups sampled.

Whole body and proximate tissue growth. Table 2 summarizes the total wet weight with age, as well as changes in lipid fraction and lean dry weight fraction for two growth scenarios. For fish from all locations, the whole body weights were linearly related to age (linear regression, $p<0.05$). The annual growth rates of fish whole body weight were higher in early life stages, and then shifted to a slower growth as fish aged. Table 2 also demonstrated the average tissue composition of Bluegill from each lake.

There were significant differences in lipid to whole body ratios among age classes for fish from Apsey Lake, Detroit River, and Stonelick Lake (ANOVA, $P<0.05$). For Apsey Lake and Detroit River, the lipid proportion was significantly higher for 0-1 years old fish compared with that of 5 year old fish; for fish from Stonelick Lake, significantly higher lipid fractions were found in 3-4 year old fish compared with 5 year olds. There were no significant differences in lean dry weight fractions between ages for fish from 4 of the 5 lake populations except for the Detroit River. In the case of the Detroit River, the lean dry weight proportion was significantly higher for 1-2 year old fish compared with 5 year old fish. The mean body mass of each age class and mean tissue to whole body ratio (across all age classes) at each location was applied to estimate daily growth of whole body, lipid and lean dry weight for scenario 1of the model simulations (Table 2). For scenario 2, the age specific tissue to whole body ratio measured for each age class of each population was applied.

Carbon and nitrogen stable isotope signature. $\delta^{15}N$ and $\delta^{13}C$ signatures of fish populations from the five waterbodies are presented in Table 1. No significant relationships were found between $\delta^{13}C$ signature and age of fish from 4 of the 5 waterbodies except for the Detroit River (linear regression, $p>0.05$) where a significantly negative relationship between $\delta^{13}C$ and age was observed. For Sharbot Lake, no significant relationship was observed between $\delta^{15}N$ signature and age (linear regression, $p>0.05$). For fish from Apsey Lake, Detroit River, and Stonelick Lake, the $\delta^{15}N$ values were positively related to age (linear regression, $p<0.05$). However, a negative relationship was observed between the $\delta^{15}N$ values and age for fish from Lake Hartwell (linear regression, $p<0.05$). Overall, the $\delta^{13}C$ signatures suggested that there might be a habitat shift for fish from Detroit River as they age, and the $\delta^{15}N$ signature suggested that there was slight trophic level shift for fish from Apsey Lake, Detroit River, Stonelick Lake, and Lake Hartwell over time. The isotope data provide support for ontogenetic diet shifts by the different fish populations which could translate into differences in prey composition and contamination as a function of fish age.

Model simulations. Hg and PCB 180 concentrations were simulated using each of the two growth scenarios and toxicokinetic parameters developed from previous studies. To examine the goodness of fit of each growth scenario model, linear regression was performed between the measured chemical concentrations and modeled chemical concentrations (only A=1.5 was considered). The chemical concentrations were log 10 transformed to conform to normal distribution. Figure 2 presents linear regressions between measured and predicted Hg and PCB 180 concentrations at each location. The linear regression equation was $y=0.9916x-0.0315$ ($R^2=0.88$) for growth scenario 1, and $y=0.988x-0.0197$ ($R^2=0.89$) for growth scenario 2 when combined across chemicals and populations. The constants of both regression were not significantly different from 0 (t-test, $p>0.05$), and the slope was not significantly different from 1(t-test, $p>0.05$), which indicated a high predictive ability of the model under both growth scenarios. Table 3 summarizes linear regression equations of measured and predicted concentrations for each chemical from each location. For Hg, the two growth scenarios provided similar results for all locations except for the Detroit River. The growth scenario 2 provided a

better prediction compared with growth scenario 1 for the latter population. For PCB 180, both growth scenarios showed relatively poor predictive power for Sharbot Lake, Detroit River, and Lake Hartwell ($p>0.05$, linear regression). However, the growth scenario 2 improved the model predictions compared with growth scenario 1 for Apsey Lake and Stonelick Lake. Thus, growth scenario 2 provided better prediction in some lake systems.

Figure 3 summarizes modeled Hg and PCB bioaccumulation trajectories and data fit using growth scenario 2. To better demonstrate the bioaccumulation trend of each population regardless of their background chemical levels, the chemical concentration of each fish was divided by the mean chemical concentration of YOY fish (C_0) from its own sampling site.

Under the simulations for Hg, $C_{0,Hg}$ was 25.12, 47.68, 103.18, 29.36, and 19.98 $ng \cdot g^{-1}$ wet weight for Apsey Lake, Sharbot Lake, Detroit River, Stonelick Lake and Lake Hartwell, respectively. Based on the best fit $C_{d,Hg}$ of each sampling site, the mean BMF ($C_{0,Hg}$ / $C_{d,Hg}$) across all locations was 1.79. Therefore, $C_{d,Hg}$ was estimated as 14.06, 26.69, 57.75, 16.44 and 11.18 $ng \cdot g^{-1}$ wet weight for Apsey Lake, Sharbot Lake, Detroit River, Stonelick Lake, and Lake Hartwell, respectively. Using 3 activity levels (Figure 3), the model was generally able to bracket field-collected Hg data for fish from Apsey Lake, Sharbot Lake, and Detroit River, but not for Stonelick Lake and Lake Hartwell. For Stonelick Lake, the model overestimated the Hg concentration for 2 year old fish, and underestimated the Hg concentration for 3-5 year old fish. For Lake Hartwell, the model underestimates Hg concentration for all age classes.

In general, the fraction of assimilated Hg retained by fish decreased with age across all locations (Table 4). The protein growth rate ($k_{g,pro}$) to total elimination rate (k_{tot}) ratio ranged from 0.02 to 0.79 for Apsey Lake, from 0.04 to 1.06 for Sharbot Lake, from 0.06 to 0.88 for Detroit River, from 0.06 to 0.80 for Stonelick Lake, and from 0.11 to 0.45 for Lake Hartwell. This indicated that growth dilution in many cases approached and in some cases exceeded the magnitude of k_{tot} implying the growth dilution is important for regulating Hg bioaccumulation compared with other elimination routes.

Under the PCB simulation, the $C_{0,PCB}$ values were 0.10, 0.18,0.54, 0.27, and 28.39 $ng \cdot g^{-1}$ wet weight, and $C_{d,PCB}$ values were estimated as 0.06, 0.10, 0.30, 0.15, and 15.89 $ng \cdot g^{-1}$ wet weight for Apsey Lake, Sharbot Lake, Detroit River, Stonelick Lake, and Lake Hartwell, respectively. The PCB simulations were generally well fitted to the field collected data for all sampling locations except for fish from the Detroit River and Lake Hartwell. For the Detroit River, the model predicted a slow increase while the field data showed a faster bioaccumulation rate. For Lake Hartwell, the model overestimated the PCB 180 concentration for all age classes.

Similar to Hg, the fraction of assimilated PCB 180 retained by fish decreased with age across all locations (Table 4). The cumulative percentage of assimilated PCB 180 retained by fish was generally higher than that of Hg for all location except for Lake Hartwell. The lipid growth rate ($k_{g,lip}$) to total elimination rate (k_{tot}) ratio ranged from -0.10 to 1.28 for Apsey Lake, from 0.09 to 2.08 for Sharbot Lake, from 0.05 to 1.36 for the Detroit River, from -0.34 to 1.46 for Stonelick Lake, and from 0.01 to 0.37 for Lake Hartwell. In general, growth dilution plays a

major role in regulating PCB bioaccumulation rates as $k_{g,lip}$ became a dominant elimination pathway (pseudoelimination) during the growing seasons ($k_{g,lip} / k_{tot} > 1$). However, growth played a less important role in PCB bioaccumulation compared with other PCB elimination pathways (i.e. chemical loss via respiration, urine, feces, and metabolic biotransformation) for fish from Lake Hartwell which had the lowest lipid content of all fish populations examined.

DISCUSSION

This study simulated Hg and PCB concentrations in Bluegill using a combined non steady state toxicokinetic and bioenergetics model. The simulations were performed under two growth scenarios. Growth scenario 1 required measurements for total growth rate, and growth scenario 2 required measurements for tissue specific growth rate. The results showed that the growth scenario 2 provided improved predictions for Hg in fish from Detroit River (44% improved R^2; Table 3), as well as for PCBs in fish from Stonelick Lake (45% improved R^2). This could be a result of high variance in protein growth rate of fish from the Detroit River and in lipid growth rate of fish from Stonelick Lake and Apsey Lake. However, the two growth scenarios were nearly identical in their predictive power for Hg and PCB from most other locations. The tissue composition from other locations did not exhibit large differences between age classes which minimized model predicted differences between the two growth scenarios. This study demonstrated that using lipid and lean dry protein growth rate could improve the accuracy of model outcomes, while previous studies usually adopt whole body growth rate in Hg and PCB bioaccumulation models (Trudel and Rasmussen, 2006; Drouillard et al. 2009). However, improvement of growth scenario 2 over scenario 1 will only be apparent in populations where proximate tissue growth shows distinct differences compared to whole body growth between age classes. Extending validation data sets to older age classes where growth performance is expected to slow even more or to lake populations experiencing resource shortage stress would be useful for further discriminating against the two growth scenarios.

In this study, the k_g / k_{tot} ratio was generally higher for PCB simulations in comparison with Hg simulations. This indicated that growth dilution was a more important process for PCB accumulation compared with Hg accumulation. In addition, $k_{g,lip}$ exhibited much higher variation compared with $k_{g,pro}$ among populations and age classes. Among the age classes of each lake, coefficients of variation for lean dry weight to whole body weight ratios were 0.09, 0.07, 0.09, 0.07, and 0.07, while coefficients of variation for lipid weight to whole body weight ratios were 0.38, 0.19, 0.43, 0.31 and 0.61 for Apsey Lake, Sharbot Lake, Detroit River, Stonelick Lake, and Lake Hartwell, respectively. Moreover, higher variabilities in PCB 180 concentration were observed in comparison with Hg concentration. Among the age classes, the coefficients of variation for Hg concentration were 0.40, 0.21, 0.22, 0.55, and 0.52, whereas the coefficients of variation for PCB concentration were 0.66, 1.21, 1.38, 0.77, and 0.47 for Apsey Lake, Sharbot Lake, Detroit River, Stonelick Lake, and Lake Hartwell, respectively. Since lean dry protein and lipid represent the storage compartments for Hg and PCB respectively, our results suggested that

high variabilities in PCB concentrations compared to Hg were partially a result of the highly variable lipid growth rates compared to protein.

Typically, lean dry protein represents a larger fraction of the total body weight of fish, whereas lipid represents a much smaller fraction of body weight and is expected to undergo wider fluctuations across ages and on a seasonal basis compared to protein (Paterson et al. 2007). Therefore, PCB concentrations in fish are expected to fluctuate much more compared with Hg concentrations in general. In this study, the goodness of fit tests for Hg were much closer to a 1:1 line compared with that of PCBs (Figure 2), which indicated that the model outcome for Hg was more accurate compared with PCB 180. This also could be attributed to higher variability in individual lipid growth within and among age classes of fish.

For the present simulations, the fish diet was estimated from YOY fish concentrations reflective of baseline inputs to each lake, and assumed to be constant across age classes in each lake. Thus, model simulations accounted for body size and temperature related changes in feeding rate and age class specific growth/proximate composition but did not consider variability in prey contamination or diet shifts with age. The constant diet assumption was based on past literature. Burtnyk et al. (2009) found no significant differences in either carbon or nitrogen stable isotope signatures between age classes (2-5) of Bluegill from Sharbot Lake. Paterson et al. (2006) observed no major shifts in diet for Bluegill from Detroit River. Overall, accounting for population specific growth and applying a constant diet concentration explained more than 80% of the variation (R^2=0.89) in chemical bioaccumulation for different age classes of Bluegill from five waterbodies (Figure 2), with a mean explained variation of 83% for Hg and 78% for PCBs, respectively.

However, the isotope data from the present study did provide evidence for dietary shifts for fish from Apsey Lake, Detroit River, Stonelick Lake, and Lake Hartwell. The changes in diet could lead to changes in prey contamination levels with age, leading to poor predictive power of the model in some of the lake systems tested. Indeed, the model generated the poorest predictions for Lake Hartwell (both contaminants) and the Detroit River (PCBs) suggesting that diet shifts and associated prey contamination changes may have been as important or more important to observed bioaccumulation rates than fish growth for these locations. In the case of PCB 180 in the Detroit River, the model fit could be improved by applying an increasing diet concentration with age than generated from the constant diet concentration used in the model simulations. In the case of Lake Hartwell, the nitrogen isotope signature suggested a decrease in trophic level with increasing age of fish, while the PCB concentrations tended to decline with age for this population.

Furthermore, Lake Hartwell and the Detroit River are also known to be contaminated systems. Thus, heterogeneous contamination across diet concentrations is more likely to occur for fish from these systems. Contaminant concentrations tend to be patchy and spatially variable at more contaminated sites, so even small scale movements by fish within the site could profoundly affect their contaminant concentrations and our ability to model them (McLeod et al.

2015). Future study on contaminant levels in Bluegill food items across age classes would be necessary to improve the model inputs, particularly for Detroit River and Lake Hartwell and to further validate the model for these populations.

Another factor not considered by our model is sex based differences in contaminant elimination. PCB elimination from females can be influenced by maternal offloading (Fisk et al. 1998; Russel et al. 1999) during spawning events. Overtime these loses can contribute to sex differences in PCB concentrations that can accumulate with age (Laesson et al. 1993). However, the role of maternal offloading to eggs varies by species. For example, Madenjian et al. (2013, 2014) highlighted sex differences in energy expenditures and foraging ranges which for some species and populations appear to play a larger role than maternal deposition to eggs. In contrast, Hg commonly exhibits the opposed pattern of sex based differences in concentration described for PCBs. Males tend to achieve lower Hg concentrations compared to females and males also show higher elimination rates of Hg compared to females suggesting a hormonal interaction with Hg elimination (Madenjian et al. 2016). Our study did not separate males from females to evaluate sex based differences in chemical concentrations nor did the model consider applying different values of k_{tot} for male and female fish for the two pollutant types. However, these modifications could be readily adopted within the model by separate model parameterization to individual sexes. In addition, fish collections from the different populations occurred at different times of the year which may have captured mature fish under different reproductive states. While this would not likely impact age-accumulated sex differences described for PCBs, it could have influenced our estimates of mean age specific proximate composition. Thus, future research to monitor both seasonal changes in proximate tissue content between ages and sexes a well as contaminant concentrations are necessary to substantiate daily and seasonal patterns in Hg and PCB bioaccumulation estimated by the model.

CONCLUSIONS

A combined toxicokinetic and bioenergetic model that accounts for population specific differences in growth was able to provide accurate prediction of age-specific Hg and PCB concentrations in Bluegill from Apsey Lake, Sharbot Lake, and Stonelick Lake. The poor performance of the model for the Detroit River and Lake Hartwell was attributed to changes in the feeding behavior of fish and associated change in prey contamination, especially for these locations with high heterogeneity in patterns of spatial contamination. Overall, growth and baseline prey contamination inferred from YOY fish concentrations, accounted for 80% of the variation in contaminant bioaccumulation across populations. In the present study, lean dry protein content was normally a constant proportion of the whole body weight of bluegill fish, whereas lipids exhibited higher seasonal and annual variation leading to discrepancies in the bioaccumulation trajectories and individual variation observed for Hg and PCBs. These results support a conclusion that age specific differences in lipid growth plays a role in explaining differences in PCB bioaccumulation rates among fish populations whereas more consistent

growth of lean dry protein contributes to less variation in bioaccumulation slopes for Hg in fish populations between systems.

Supplemental Data

Information regarding the procedures for THg, PCBs, nitrogen and carbon stable isotope analysis, age determination, as well as water temperature sub-model development is available on the Wiley Online Library. Supplemental information are included with this accepted manuscript publication.

Acknowledgements

We are grateful to M. Dufour, S. Hsu, N. Ismail, and J. C Barrette for their assistance with laboratory analysis. Scholarship funding was provided by the China Scholarship Council grant to J. Li. This study was funded by CRC and OCRIF grants to G. D. Haffner, as well as by NSERC discovery grant to K. G. Drouillard.

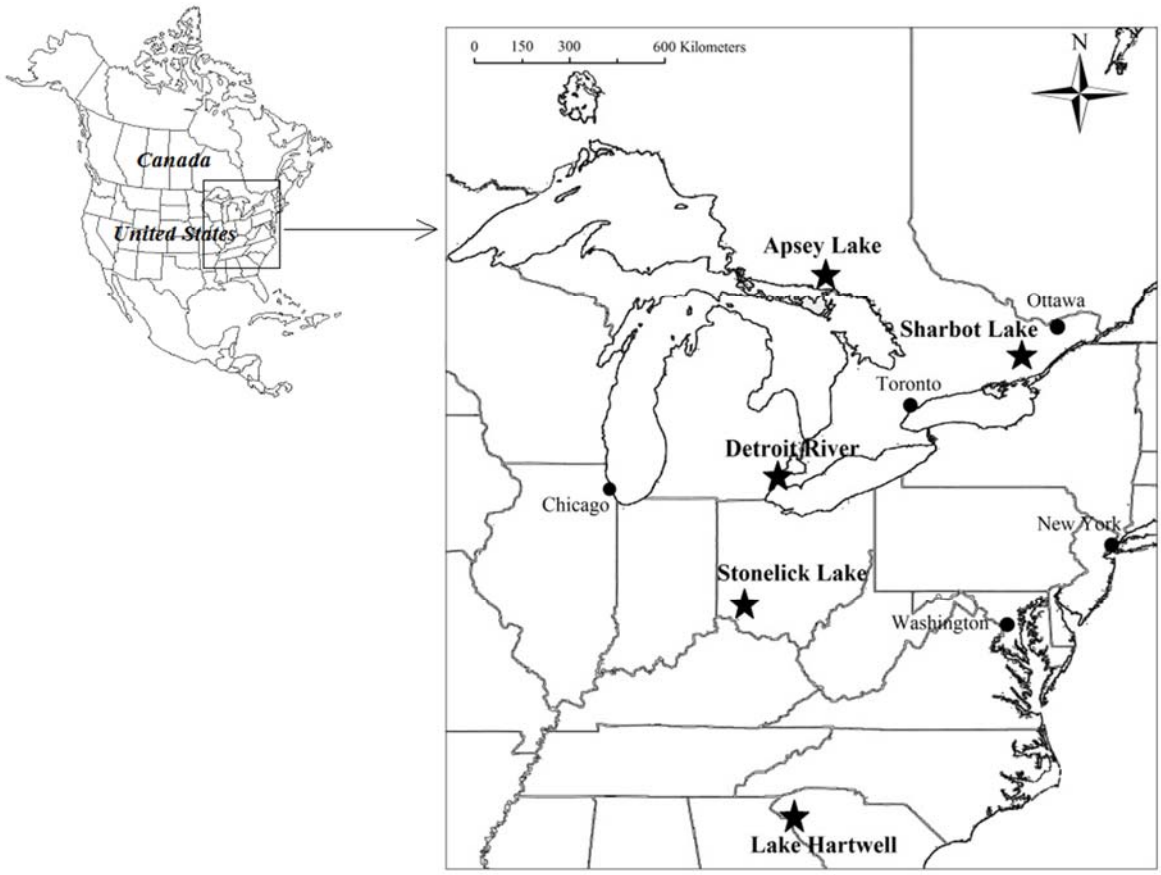

Figure 1. Map of sampling location. Stars represent sampling sites.

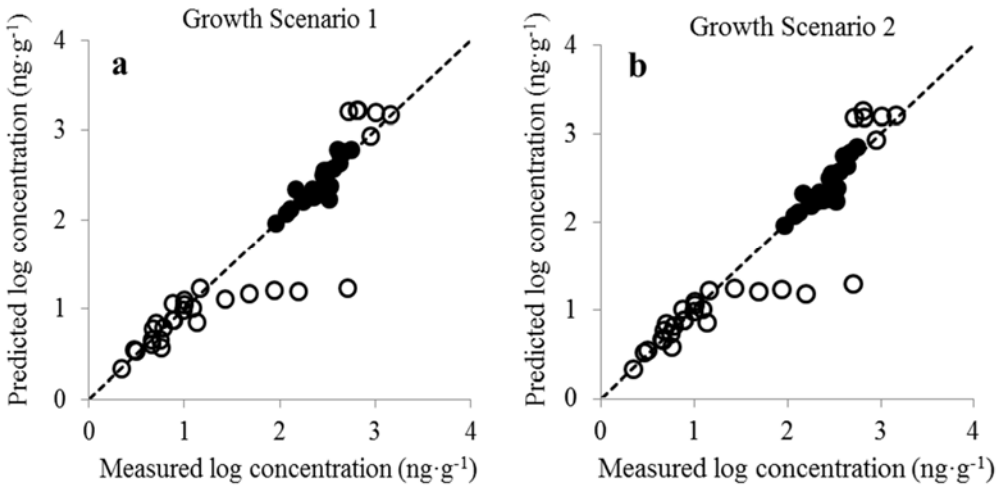

Figure 2. Relationships between predicted and observed Hg and PCB180 concentrations across lake populations and age classes under model assumptions of; (a) lipid and protein growth rates proportional to whole body growth (Scenario 1) and; (b) population specific lipid and protein growth rates (Scenario 2). In both panels, solid (●) and open (○) symbols represent Hg and PCB 180, respectively. Dashed line represents the 1:1 regression fit.

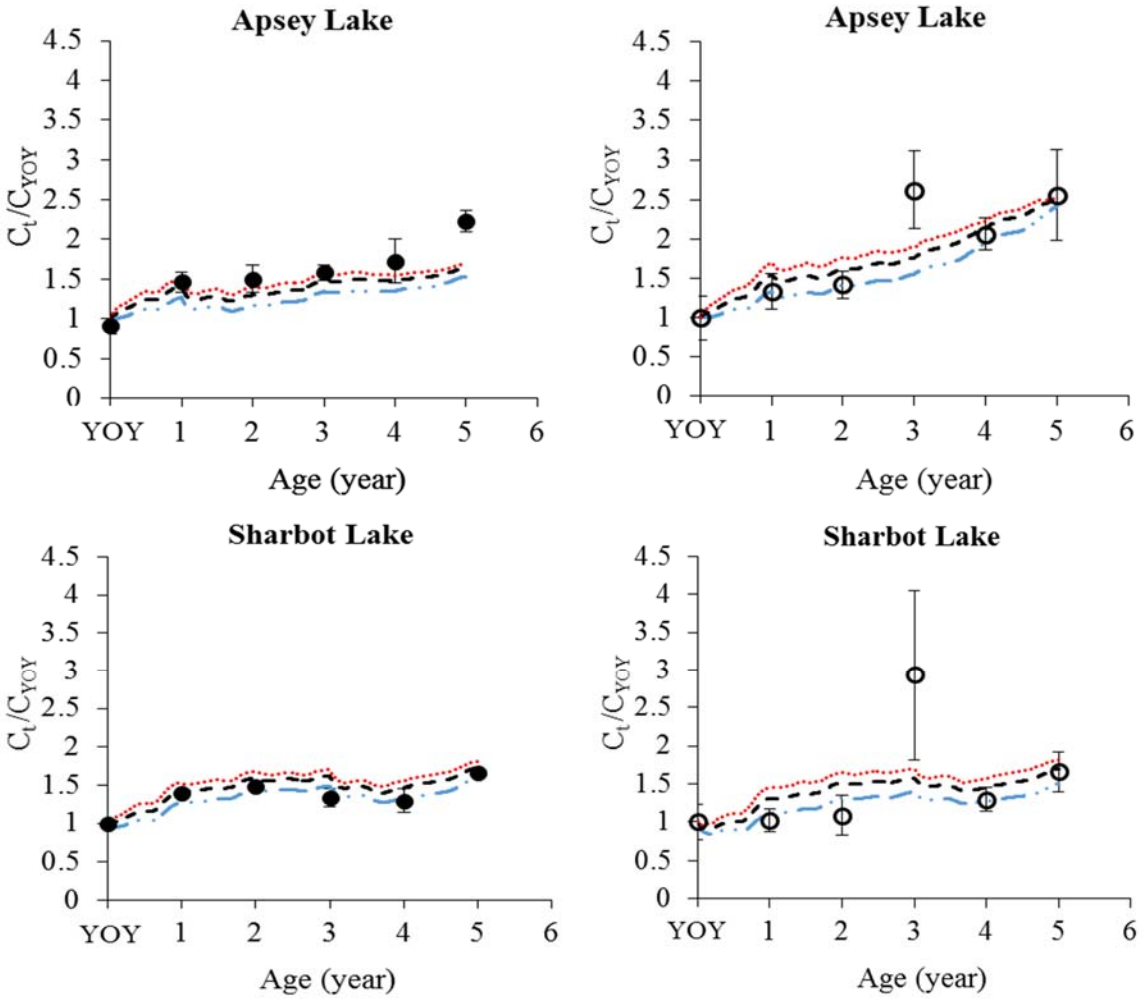
Apsey Lake
Apsey Lake
Sharbot Lake
Sharbot Lake
C_t/C_{YOY}
Age (year)
YOY
0
0.5
1
1.5
2
2.5
3
3.5
4
4.5
5
6

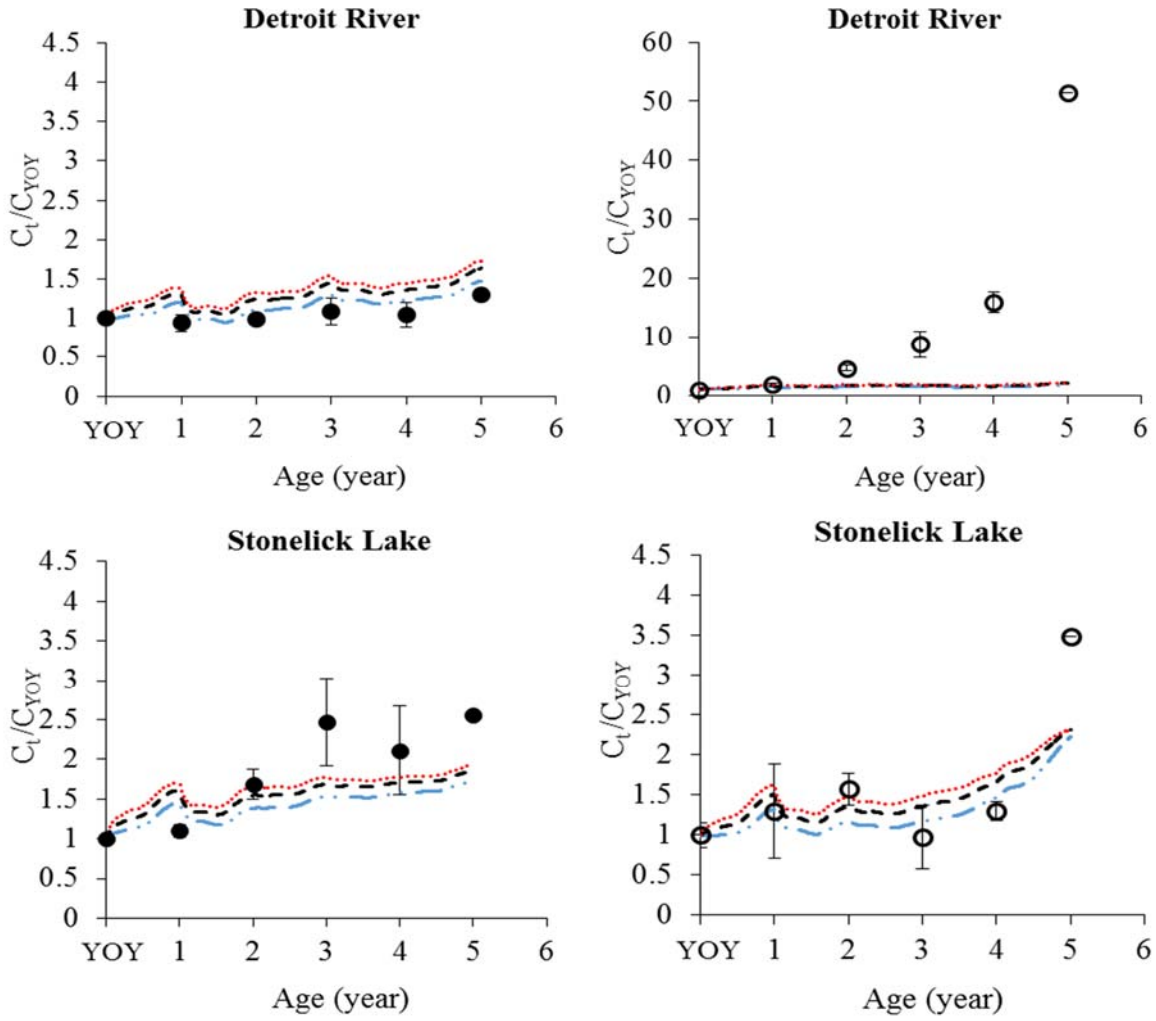
Detroit River
Detroit River
Stonelick Lake
Stonelick Lake
C_t/C_{YOY}
Age (year)
YOY
0
0.5
1
1.5
2
2.5
3
3.5
4
4.5
10
20
30
40
50
60
1
2
3
4
5
6

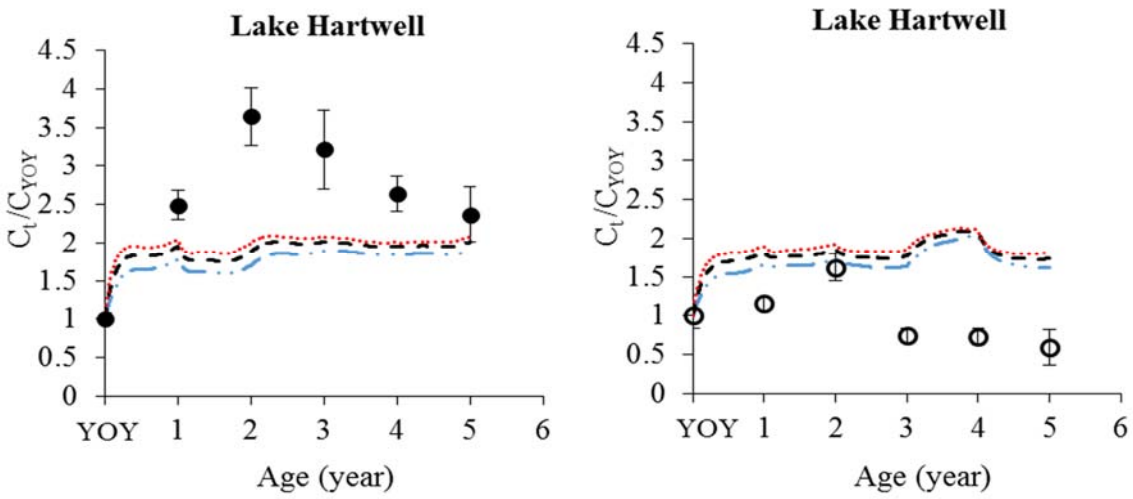

Figure 3. Relationship between relative chemical level (chemical concentration in fish [Ct] divided by chemical concentration in YOY [C_{YOY}]) and age for individual lake populations. Solid circles (●) (●) represent THg and open circles (○) represent PCB 180. Error bars used standard error; dashed lines (---) represent the modeled concentrations at activity levels = 1 (blue), 1.5 (black), and 2 (red), respectively.

Table 1. Summarized biological data, THg concentrations, sum PCB (ΣPCB) concentrations, $\delta^{13}C$ and $\delta^{15}N$ signatures for Bluegill collected from five sampling locations across North America. Values represent mean ± 1 standard error with data minima and maxima included in parentheses.

Sampling Location (n)	Total Length (mm)	Mass (g)	THg		ΣPCB		$\delta^{15}N$	$\delta^{13}C$
			($ng \cdot g^{-1}$ wet wt)	($ng \cdot g^{-1}$ LDW[a])	($ng \cdot g^{-1}$ wet wt)	($ng \cdot g^{-1}$ lipid)	(‰)	‰
Apsey Lake (41)	7.5 ± 0.4 (3.3 – 12.5)	9.6 ± 1.1 (0.4 – 32.8)	38.6 ± 1.9 (16.4 – 102.3)	171.6 ± 8.5 (72.8 – 285.1)	4.2 ± 0.6 (1.1 – 24.6)	103.8 ± 18.6 (21.6– 765.6)	8.4 ± 0.5 (7.3 – 9.2)	-20.3 ± 1.1 (-22.5 – -18.4)
Sharbot Lake (47)	7.8 ± 0.4 (3.6 – 15.5)	10.4 ± 1.5 (0.6 – 57.2)	62.7 ± 1.6 (34.7 – 90.8)	289.0 ± 8.9 (153.9 – 422.0)	4.6 ± 1.0 (ND[b] – 44.2)	88.6 ± 17.3 (ND – 749.7)	9.3 ± 0.5 (8.2 – 10.1)	-28.1 ± 1.4 (-29.3 – -23.9)
Detroit River (54)	8.5 ± 0.5 (2.6 – 18.3)	18.5 ± 3.3 (0.2 – 130.9)	101.9 ± 3.0 (61.0 ± 153.9)	433.7 ± 14.0 (246.4 – 680.0)	26.2 ± 2.8 (4.4 – 104.3)	604.6 ± 70.1 (95.7 – 2916)	10.7 ± 0.9 (9.2 – 13.1)	-16.0 ± 3.0 (-22.5 – -11.1)
Stonelick Lake (47)	8.2 ± 0.6 (2.9 – 17.3)	17.9 ± 3.3 (0.2 – 100.0)	41.8 ± 3.2 (22.3 – 160.1)	188.6 ± 14.2 (96.6 – 606.1)	7.2 ± 1.3 (ND – 17.1)	206.1 ± 41.7 (ND – 2012)	11.8 ± 0.6 (10.5 – 12.9)	-25.8 ± 0.7 (-27.1 – -24.5)
Lake Hartwell (62)	9.6 ± 0.4 (4.6 – 15.8)	16.9 ± 2.0 (1.4 – 68.0)	54.7 ± 3.6 (14.3 – 150.8)	244.7 ± 15.6 (66.9 – 635.8)	1411.7 ± 100.3 (115.7 – 4020)	12362 ± 2702 (5764 – 1.1 x 10^5)	10.6 ± 1.2 (8.5 – 12.1)	-25.9 ± 1.5 (-29.5 – -22.5)

[a] LDW indicates lean dry weight.
[b] ND represents non-detect.

Table 2. Measured total mass (Mean±SE), lipid to whole body weight ratio (Mean±SE), and lean dry weight (LDW) to whole body weight ratio (Mean±SE) for fish of each age class from each location.

Site	Age	All ages	YOY	1	2	3	4	5
		(Scenario 1)	(Scenario 2)					
Apsey Lake	Sample size	41	11	6	5	13	3	3
	Mass (g)	--	0.78±0.13	2.75±0.09	8.41±0.77	15.44±0.69	21.48±1.20	24.94±2.69
	Lipid (%)	3.28±0.19	4.18±0.22	3.87±0.51	3.08±0.59	2.98±0.29	2.20±0.69	1.48±0.25
	LDW (%)	22.51±0.33	21.51±0.21	22.73±0.67	23.93±1.73	22.13±0.44	24.17±2.22	23.32±0.51
Sharbot Lake	Sample size	47	10	15	6	10	4	2
	Mass (g)	--	0.92±0.06	5.62±0.42	11.05±0.39	19.07±1.31	45.15±2.51	56.40±0.80
	Lipid (%)	3.95±0.75	3.90±0.15	4.10±0.23	4.06±0.16	3.95±0.31	3.55±0.38	3.64±0.61
	LDW (%)	22.30±0.22	21.68±0.15	22.84±0.44	22.25±0.35	22.23±0.70	22.26±0.47	21.98±1.14
Detroit River	Sample size	54	9	11	25	5	3	1
	Mass (g)	--	1.34±0.15	3.86±0.32	18.48±1.11	39.66±2.54	85.10±2.67	130.9
	Lipid (%)	3.72±0.22	5.08±0.41	4.41±0.60	2.99±0.24	2.96±0.72	3.58±0.21	2.57
	LDW (%)	23.81±0.30	23.50±0.57	25.73±0.93	24.24±0.38	22.00±0.91	22.92±1.01	20.04
Stonelick Lake	Sample size	47	21	6	12	5	2	1
	Mass (g)	--	1.58±0.19	6.37±0.81	28.39±1.82	51.44±2.45	75.50±3.4	100
	Lipid (%)	3.40±0.15	3.22±0.13	3.24±0.27	3.38±0.33	4.63±0.85	3.78±0.0003	1.62
	LDW (%)	22.92±0.24	22.29±0.24	23.88±0.55	23.08±0.54	23.31±1.28	24.05±0.02	22.53

Lake Hartwell	Sample size	62	9	25	15	7	2	4
	Mass (g)	--	2.49±0.18	6.72±0.47	20.98±0.97	30.67±1.88	41.65±1.45	61.53±2.31
	Lipid (%)	1.78±0.14	2.27±0.39	1.92±0.23	1.17±0.19	2.00±0.40	1.20±0.80	2.06±0.65
	LDW (%)	22.47±0.21	21.88±0.55	22.58±0.30	22.10±0.53	23.03±0.53	24.10±0.74	22.72±0.73

Table 3. Linear regression between predicted and observed Hg and PCB180 concentrations under two growth scenarios.

Sampling site	Chemical	Growth scenario 1						Growth scenario 2					
		β (slope)			α (intercept)		R square	β (slope)			α (intercept)		R square
		Value	SE	p	Value	SE		Value	SE	p	Value	SE	
Apsey Lake	Hg	0.680	0.084	0.001	0.682	0.191	0.942	0.621	0.102	0.004	0.803	0.231	0.903
	PCB	0.542	0.174	0.035	0.230	0.103	0.709	0.696	0.204	0.027	0.167	0.121	0.745
Sharbot Lake	Hg	1.052	0.198	0.006	-0.098	0.49	0.876	1.068	0.203	0.006	-0.138	0.502	0.874
	PCB	0.264	0.178	0.214	0.594	0.146	0.353	0.274	0.181	0.205	0.589	0.148	0.364
Detroit River	Hg	0.331	0.534	0.569	1.861	1.419	0.088	1.041	0.505	0.108	-0.014	1.343	0.515
	PCB	0.085	0.059	0.220	1.022	0.11	0.345	0.12	0.057	0.104	0.979	0.107	0.525
Stonelick Lake	Hg	0.413	0.185	0.090	1.337	0.437	0.554	0.421	0.168	0.067	1.31	0.397	0.61
	PCB	0.218	0.176	0.282	0.813	0.186	0.279	0.508	0.152	0.029	0.525	0.162	0.735
Lake Hartwell	Hg	0.558	0.14	0.016	0.907	0.329	0.798	0.551	0.123	0.011	0.917	0.289	0.834
	PCB	-0.179	0.331	0.617	3.687	0.963	0.068	-0.076	0.35	0.839	3.388	1.018	0.012

Table 4. Fraction of Hg and PCB retained in fish for each age class under the model simulation

		Scenario 1		Scenario 2	
Location	age	Hg retained %	PCB retained %	Hg retained %	PCB retained %
Apsey Lake	1	32.19	44.09	32.32	46.51
	2	30.65	41.12	30.55	39.52
	3	25.5	35.27	25.69	32.55
	4	19.28	27.78	19.38	20.04
	5	12.74	19.53	12.89	3.70
	All age	20.76	29.33	20.91	21.39
Sharbot Lake	1	35.02	49.23	34.96	50.06
	2	23.56	36.26	23.56	36.76
	3	20.7	31.81	20.73	31.62
	4	27.75	39.58	27.89	37.02
	5	18.97	30.41	19.06	28.33
	All age	23.37	35.16	23.45	33.63
Detroit River	1	26.15	39.65	25.96	42.37
	2	32.29	44.59	32.59	39.66
	3	26.74	38.52	27.22	33.45
	4	27.43	38.86	27.49	39.05
	5	23.17	34.02	23.85	25.65
	All age	25.95	37.28	26.42	32.73
Stonelick Lake	1	29.23	38.99	29.24	38.43
	2	31.4	41.96	31.4	42.01
	3	22.98	32.46	22.64	39.5
	4	17.73	25.65	17.61	27.95
	5	14.53	21.25	14.86	1.4
	All age	19.73	27.91	19.84	23.09
Lake Hartwell	1	24.6	23.95	24.73	24.33
	2	23.9	23.94	24.1	17.71
	3	14.53	14.1	14.45	17.89
	4	11.04	10.76	11	6.37
	5	12.86	12.72	12.83	16.4
	All age	15.02	14.78	14.99	14.96

RERERENCES

Arnot JA, Gobas FAPC. 2004. A food web bioaccumulation model for organic chemicals in aquatic ecosystems. *Environ. Toxicol. Chem.* 23: 2343-2355. DOI: 10.1897/03-438.

Berg OK, Bremset G. 1998. Seasonal changes in the body composition of young riverine Atlantic salmon and brown trout. *J. Fish Biol.* 52(6): 1272-1288. DOI:10.1006/jfbi.1998.0679.

Bloom NS. 1992. On the chemical form of mercury in edible fish and marine invertebrate tissue. *Can. J. Fish Aquat. Sci.* 49: 1010-1017. DOI: 10.1139/f92-113.

Burtnyk MD, Paterson G, Drouillard KG, Haffner GD. 2009. Steady and non-steady state kinetics describe polychlorinated biphenyl bioaccumulation in natural populations of Bluegill (*Lepomis macrochirus*) and cisco (*Coregonus artedi*). *Can. J. Fish. Aquat. Sci.* 66: 2189-2198. DOI: 10.1139/F09-150.

Bzdusek PA, Christensen ER, Lee CM, Pakdeesusuk U, Freedman DL. 2006. PCB congeners and dechlorination in sediments of Lake Hartwell, South Carolina, determined from cores collected in 1987 and 1998. *Environ. Sci. Technol.* 40(1): 109-119. DOI: 10.1021/es050194o.

Daley JM, Paterson G, Drouillard KG. 2014. Bioamplification as a bioaccumulation mechanism for persistent organic pollutants (POPs) in wildlife. *Rev. Environ. Contam. Toxicol.* 227: 107-155. DOI: 10.1007/978-3-319-01327-5_4.

Debruyn AMH, Gobas FAPC. 2007. The sorptive capacity of animal protein. *Environ. Toxicol. Chem.* 26: 1803-1808. DOI: 10.1897/07-016R.1.

Drouillard KG, Paterson G, Haffner GD. 2009. A combined food web toxicokinetic and species bioenergetic model for predicting seasonal PCB elimination by yellow perch (*Perca flavescens*). *Environ. Sci. Technol.* 43(8): 2858-2864. DOI: 10.1021/es802567p.

Drouillard KG, Tomczak M, Reitsma S, Haffner GD. 2006. A river-wide survey of polychlorinated biphenyls (PCBs), polycyclic aromatic hydrocarbons (PAHs), and selected organochlorine pesticide residues in sediments of the Detroit River—1999. *J. Great Lakes Res.* 32: 209-226. DOI: https://doi.org/10.3394/0380-1330(2006)32[209:ARSOPB]2.0.CO;2.

Fisk AT, Johnston TA. 1998. Maternal transfer of organochlorines to eggs of walleye (*Stizostedion vitreum*) in Lake Manitoba and western Lake Superior. *J. Great Lakes Res.* 24 (4): 917-928. DOI: 10.1016/S0380-1330(98)70872-X.

Gobas FAPC, Wilcockson JB, Russell RW, Haffner GD. 1999. Mechanism of biomagnification in fish under laboratory and field conditions. *Environ. Sci. Technol.* 33: 133-141. DOI: 10.1021/es980681m.

Gobas FAPC, Zgraggen MN, Zhang X. 1995. Time response of the Lake Ontario ecosystem to virtual elimination of PCBs. *Environ. Sci. Technol.* 29: 2038-2046. DOI: 10.1021/es00008a024.

Hall BD, Bodaly RA, Fudge RJP, Rudd JWM, Rosenberg DM. 1997. Food as the dominant pathway of methylmercury uptake by fish. *Water, Air, and Soil Pollut.* 100: 13-24. DOI: https://doi.org/10.1023/A:1018071406537.

Hanson PC, Johnson TB, Schindler DE, Kitchell JF. 1997. "Fish Bioenergetics 3.0." University of Wisconsin Sea Grant Institute, Madison, Wisconsin.

Holker F, Haertel SS. 2004. Application of a bioenergetics model to roach. *J. Appl. Ichthyol.* 20(6): 548-550. DOI: 10.1111/j.1439-0426.2004.00586.x.

Kitchell JF, Stewart DJ, Weininger D. 1977. Applications of a bioenergetics model to yellow perch (*Perca flavescens*) and walleye (*Stizostedion vitreum vitreum*). *J. Fish. Res. Bd. Can.* 34(10): 1922-1935. DOI: https://doi:.org/10.1139/f77-258.

Larsson P, Okla L, Collvin L. 1993. Reproductive status and lipid content as factors in PCB, DDT, and HCH contamination of a population of pike (*Esox lucius L.*). *Environ. Toxicol. Chem.* 12 (5): 855–861. DOI: 10.1897/1552-8618(1993)12[855:RSALCA]2.0.CO;2.

Leaner JJ, Mason RP. 2004. Methylmercury uptake and distribution kinetics in sheepshead minnows, *Cyprinodon variegatus*, after exposure to CH_3Hg-spiked food. *Environ. Toxicol. Chem.* 23(9): 2138-2146. DOI: 10.1897/03-258.

Li J, Drouillard KG, Branfireun B, Haffner GD. 2015. Comparison of the toxicokinetics and bioaccumulation potential of mercury and polychlorinated biphenyls in goldfish (*Carassius auratus). Environ. Sci. Technol.* 49: 11019-11027. DOI: 10.1021/acs.est.5b02727.

Liu J, Haffner GD, Drouillard KG. 2010. The influence of diet on the assimilation efficiency of 47 polychlorinated biphenyl congeners in Japanese Koi (*Cyprinus carpio*). *Environ. Toxicol. Chem.* 29: 401-409. DOI: 10.1002/etc.47.

Mackay D. 1982. Correlation of bioconcentration factors. *Environ. Sci. Technol.* 16(5): 274-278. DOI:10.1021/es00099a008.

Madenjian CP, O'Connor DV, Pothoven SA, Schneeberger PJ, Rediske RR, O'Keefe JP, Bergstedt RA, Argyle RL, Brandt SB. 2006. Evaluation of a lake whitefish bioenergetics model. *Trans. Am. Fish. Soc.* 135(1): 61-75. DOI: 10.1577/T04-215.1.

Madenjian CP, Johnson NS, Binder TR, Rediske RR, O'Keefe JP. 2013. Polychlorinated biphenyl concentrations and activity of sea lamprey Petromyzon marinus vary by sex. *Arch. Environ. Contam. Toxicol.* 65: 693–703. DOI: 10.1007/s00244-013-9936-y.

Madenjian CP, Yule DL, Chernyak SM, Begnoche LJ, Berglund EK, Isaac EJ. 2014. Males exceed females in PCB concentrations of cisco (*Coregonus artedi*) from Lake Superior. *Sci. Total Environ.* 493:377-83. DOI: 10.1016/j.scitotenv.2014.06.007.

Madenjian CP, Rediske RR, Krabbenhoft DP, Stapanian MA, Chernyak SM, O'Keefe JP. 2016. Sex differences in contaminant concentrations of fish: a synthesis. *Biology of Sex Differences.* 7: 42. DOI: 10.1186/s13293-016-0090-x.

Mason RP, Reinfelder JR, Morel FMM. 1995. Bioaccumulation of mercury and methylmercury. *Water, Air, and Soil Pollut.* 80: 915-921. DOI: 10.1007/BF01189744.

McIntyre JK, Beauchamp DA. 2007. Age and trophic position dominate bioaccumulation of mercury and organochlorines in the food web of Lake Washington. *Sci. Tot. Env.* 372: 571-584. DOI: 10.1016/j.scitotenv.2006.10.035.

McKim JM, Schmieder PK, Veith GD. 1985. Absorption dynamics of organic chemical transport across trout gills as related to octanol-water partition coefficient. *Toxicol. Appl. Pharmacol.* 77: 1-10. DOI: 10.1016/0041-008X(85)90262-5.

McLeod AM, Arnot JA, Borgå K, Selck H, Kashian DR, Krause A, Paterson G, Haffner GD, Drouillard KG. 2015. Quantifying uncertainty in the trophic magnification factor related to spatial movements of organisms in a food web. *Integr. Environ. Assess. Manag.* 11(2): 306-18. DOI: 10.1002/ieam.1599.

McLeod AM, Paterson G, Drouillard KG, Haffner GD. 2016. Ecological implications of steady state and nonsteady state bioaccumulation models. *Environ. Sci. Technol.* 50: 11103-11111. DOI: 10.1021/acs.est.6b03169.

Norstrom RJ, McKinnon AE, DeFreitas ASW. 1976. Bioenergetics-based model for pollutant accumulation by fish simulation of PCB and methylmercury residue levels in Ottawa River yellow perch (*Perca flavescens*). *J. Fish. Res. Bd. Can.* 33: 248-267. DOI: 10.1139/f76-035.

Overturf K, Barrows FT, Hardy RW, Brezas A, Dumas A. 2016. Energy composition of diet affects muscle fiber recruitment, body composition, and growth trajectory in rainbow trout (*Oncorhynchus mykiss*). *Aquaculture.* 457: 1-14. DOI: 10.1016/j.aquaculture.2016.02.002.

Paterson G, Drouillard KG, Haffner GD. 2006. An evaluation of stable nitrogen isotopes and polychlorinated biphenyls as bioenergetic tracers in aquatic systems. *Can. J. Fish. Aquat. Sci.* 63: 628-641. DOI: 10.1139/F05-241.

Paterson G, Drouillard KG, Haffner GD. 2007. PCB elimination by yellow perch (*Perca flavescens*) during an annual temperature cycle. *Environ. Sci. Technol.* 41: 824-829. DOI: 10.1021/es060266r.

Paterson G, Drouillard KG, Leadley TA, Haffner GD. 2007. Long-term polychlorinated biphenyl elimination by three size classes of yellow perch (*Perca flavescens*). *Can. J. Fish. Aquat. Sci.* 64: 1222-1233. DOI: 10.1139/F07-088.

Ricker WE. 1979. Growth rates and models. In Hoar WS, Randall DJ, Brett JR, eds, *Fish physiology*. Academic Press, New York. US. Pp 677-743.

Roesijadi G.1992. Metallothioneins in metal regulation and toxicity in aquatic animals. *Aquat. Toxicol.* 22(2): 81-114. DOI: 10.1016/0166-445X(92)90026-J.

Russell RW, Gobas FAPC, Haffner GD. 1999. Maternal transfer and in ovo exposure of organochlorines in oviparous organisms: A model and field verification. *Environ. Sci. Technol.* 33 (3): 416-420. DOI: 10.1021/es9800737.

Simoneau M, Lucotte M, Garceau S, Laliberte D. 2005. Fish growth rates modulate mercury concentrations in walleye (*Sander vitreus*) from eastern Canadian lakes. *Environ. Res.* 98(1): 73-82. DOI: 10.1016/j.envres.2004.08.002.

Szalinska E, Drouillard KG, Fryer B, Haffner GD. 2006. Distribution of Heavy Metals in Sediments of the Detroit River. *J. Great Lakes Res.* 32: 442-454. DOI: https://doi.org/10.3394/0380-1330(2006)32[442:DOHMIS]2.0.CO;2.

Trudel M, Rasmussen JB. 1997. Modeling the elimination of mercury by fish. *Environ. Sci. Technol.* 31: 1716-1722. DOI: 10.1021/es960609t.

Trudel M, Rasmussen JB. 2001. Predicting mercury concentration in fish using mass balance models. *Ecol. Appl.* 11: 517-529. DOI: 10.1890/1051-0761(2001)011[0517:PMCIFU]2.0.CO;2.

Trudel M, Rasmussen JB. 2006. Bioenergetics and mercury dynamics in fish: a modelling perspective. *Can. J. Fish. Aquat. Sci.* 63: 1890-1902. DOI: 10.1139/F06-081.

Watanabe KH, Desimone FW, Thiyagarajah A, Hartley WR, Hindrichs AE. 2003. Fish tissue quality in the lower Mississippi River and health risks from fish consumption. *Sci. Tot. Env.* 302: 109-126. DOI: 10.1016/S0048-9697(02)00396-0.

SUPPLEMENTARY MATERIAL

Laboratory analysis

THg concentrations were determined using a Direct Mercury Analyzer (DMA-80, Milestone Inc.). A 10 point calibration curve, using a certified standard (High-Purity Standards, Charleston, USA), was used for calibrating the instrument. Approximately 0.20 g fish homogenate was weighed on a clean nickel boat, and then placed on an autosampler. Method blanks, certified reference tissues (Dorm-3 and Dolt-4, National Research Council Canada), and in house standards (BT-Cnt2L and W-CntVG) were also analyzed for every 30 samples as quality assurance. Sample moisture contents were determined gravimetrically. The mean relative percent from deviation from duplicates was 7±5%, and recoveries averaged 95±7%

PCB concentrations were determined using an Agilent 6890 Series Plus gas chromatograph (GC) equipped with a 63Ni-micro electron capture detector and an Agilent 7683 auto sampler and a 60 m × 0.25 mm × 0.10 µm DB-5 capillary column. The PCB analysis method is described in Li et al. (2015). Approximately 0.5 g of whole fish homogenate was weighed, and added to a glass mortar with 15g of activated Na_2SO_4. After being ground with a glass pestle, the mixture was packed into a micro extraction column with 25 mL of 1:1 mixture of dichloromethane:hexane (DCM:HEX) extraction solvent. Each column was spiked with 35 ng PCB 34 as a recovery standard. The column was eluted after one hour, followed by adding another 15 mL of DCM:HEX. Sample lipid contents were determined gravimetrically using 10% of the extraction volume. Clean-up of sample was completed by activated Florisil, followed by concentration to a volume of 1 mL for GC-ECD analysis. Internal standard (PCB34), a method blank (sodium sulfate) and an in-house tissue reference sample (Detroit River carp [*Cyprinus carpio*]) were also co-analyzed for every six samples as quality assurance. The PCB concentration of each sample was corrected by its corresponding method blank. The mean relative percent difference from the in-house tissue reference sample was 16±9%, and PCB 34 recoveries averaged 73±15%.

The stable isotopes analysis method was described in Burtnyk et al. (2009). An elemental analyzer (Costech, Valencia, CA, USA) as well as a ThermoFinnigan Delta^{Plus} mass spectrometer (ThermoFinnigan, San Jose, CA, USA) were used for determination of $\delta^{15}N$ and $\delta^{13}C$ values. Approximately 1 g of whole fish homogenate was freeze-dried for 48 h, then ground into a fine powder with a glass mortar and pestle. Lipids were removed by 2:1 *v/v* chloroform:methanol. Then, the sample was allowed to dry in the fume hood with the caps removed for 24-48 hrs. Approximately 2 mg of the dried and lipid extracted material was weighed and put into a tin capsule. Ratios (R) of heavy to light nitrogen or carbon in the sample relative to that of the standard material was calculated as follows: $\delta^{15}N$ or $^{13}C = 1000 * [R_{sample} \cdot R_{standard}^{-1}-1]$ ($R = {}^{15}N:{}^{14}N$ or $^{13}C:{}^{12}C$). An internal lab standard of tilapia muscle and also NIST1577c (standard bovine liver) reference material were also analyzed for every 10 samples. The mean differences from the certified values were ≤ 0.14 ‰ and ≤ 0.04 ‰ for $\delta^{15}N$ and $\delta^{13}C$, respectively.

Age determination. The procedures for age determination are described in Burtnyk et al. (2009). The sagittal otoliths were removed from individual fish, then cleaned by forceps and distilled water. The otoliths were polished from both anterior and posterior directions toward the core using coarse (120 grit, 115 mm) and fine (3 mm) sandpaper (Ali Industries Incorporated, Fairborn, Ohio) until the annuli were readable under microscope. Fish age was determined by counting the annuli on the otolith of each fish. All otoliths were evaluated double blind by three individuals to avoid bias. Literature-based length at age ranges for Bluegill (Scott and Crossman, 1973) were also used for age estimation when there were discrepancies among the readers. For fish where no annulus could be identified from the otolith, age was defined as young of the year (YOY).

Water temperature sub-model

Annual water temperature cycle was estimated for each of the five waterbodies based on local air temperature, due to the unavailability of *in situ* field data. Daily air temperatures from Nov. 2015 to Oct. 2016 in the closest city for each lake were obtained from on-line weather reports. Since the littoral zone responds faster to air temperature changes than the whole lake and Bluegill are mainly present in this area (McCobie, 1959; Wilson et al. 1996), average air temperature over 10 days was used as a proxy of littoral water temperature with some modification. The maximum and the minimum water temperature was each set to 28 °C and 1 °C, respectively. A polynomial function was fitted to the 10 d averaged temperature pattern for the 2015-2016 annual cycle for each lake, and then the function was used to predict daily water temperature within a year. The daily water temperature curve was repeated for five years to generate a five year littoral water temperature profile for each lake. The sampling date of each lake was set to day 0 for the corresponding lake simulations.

References

Li, J., Drouillard, K. G., Branfireun, B., and Haffner, G. D. 2015.Comparison of the toxicokinetics and bioaccumulation potential of mercury and polychlorinated biphenyls in goldfish (*Carassius auratus). Environ. Sci. Technol.* 49: 11019-11027; doi: 10.1021/acs.est.5b02727.

Burtnyk, M. D., Paterson, G., Drouillard, K. G., and Haffner, G. D. 2009. Steady and non-steady state kinetics describe polychlorinated biphenyl bioaccumulation in natural populations of Bluegill (*Lepomis macrochirus*) and cisco (*Coregonus artedi*). *Can. J. Fish. Aquat. Sci.* 66: 2189-2198. doi: 10.1139/F09-150.

Scott, W. B., and Crossman, E. J. 1973. Freshwater fishes of Canada. *Bull. Fish. Res. Board Can.* No. 184.

McCombie, A. M. 1959. Some relations between air temperatures and the surface water temperatures of lakes. *Limnol. Oceanogr.* 4(3): 252-258. doi: 10.4319/lo.1959.4.3.0252.

Wilson, D. S., Muzzall, P. M., and Ehlinger, T. J. 1996. Parasites, morphology, and habitat use in a Bluegill sunfish (*Lepomis macrochirus*) population. *Copeia.* 2: 348-354. doi: 10.2307/1446850.